Rotating magnetizations in electrical machines: Measurements and modeling

Andreas Thul, Simon Steentjes, Benedikt Schauerte, Piotr Klimczyk, Patrick Denke, and Kay Hameyer

Citation: AIP Advances **8**, 056815 (2018);
View online: https://doi.org/10.1063/1.5007751
View Table of Contents: http://aip.scitation.org/toc/adv/8/5
Published by the American Institute of Physics

AIP ADVANCES **8**, 056815 (2018)

Rotating magnetizations in electrical machines: Measurements and modeling

Andreas Thul,[1,a] Simon Steentjes,[1] Benedikt Schauerte,[1] Piotr Klimczyk,[2] Patrick Denke,[2] and Kay Hameyer[1]
[1]*Institute of Electrical Machines, RWTH Aachen University, D-52062 Aachen, Germany*
[2]*Brockhaus Measurements, D-58507 Luedenscheid, Germany*

(Presented 8 November 2017; received 2 October 2017; accepted 18 December 2017; published online 18 January 2018)

This paper studies the magnetization process in electrical steel sheets for rotational magnetizations as they occur in the magnetic circuit of electrical machines. A four-pole rotational single sheet tester is used to generate the rotating magnetic flux inside the sample. A field-oriented control scheme is implemented to improve the control performance. The magnetization process of different non-oriented materials is analyzed and compared. https://doi.org/10.1063/1.5007751

I. INTRODUCTION

The increasing requirements for modern high performance electrical machines call for suitable loss and magnetization models for the highly utilized soft magnetic materials. Current approaches to this problem aim for a vectorial description of the magnetizing process, which is capable to accurately predict the hysteretic nature of these materials.[1,2] Although concepts for two-dimensional measurement devices, referred to as rotational single sheet testers (RSST), are known,[3,4] their usage is not very common compared to unidirectional methods.[5] Reasons for this might be the more complicated control of rotational magnetizations. Therefore, most models are based on unidirectional measurement data and occurring rotating flux in the later application is treated e.g. by introducing correction factors. Only few efforts have been made so far to use RSST measurements, e.g. for loss model parametrization.[6] In this work, RSST measurements are used for a more comprehensive examination. By analyzing the effects of rotational flux on different materials, a better understanding of the material behavior can be achieved. This knowledge can then be used in the machine design process to take advantage of specific material properties.

In the next section, the used measurement system and proposed control strategy are explained. Afterwards, measurements results are presented and discussed. The paper concludes with a summary of the main results.

II. RSST MEASUREMENT SYSTEM

The used four pole RSST measurement system is shown in fig. 1. A rotating magnetic field is generated by four excitation coils with 45 windings. The coils are placed on four magnetizing poles connected by a back iron. A quadratic sample (width 60 mm) is placed in the center of the four magnetizing poles. The thickness of the yoke system is large compared to the sample thickness (0.5 mm) to keep the induction values small in the yoke and thus reducing the necessary magnetizing currents. The coils are supplied by linear amplifiers (maximum current amplitude 50 A). The magnetic flux density inside the sample is measured by two perpendicular windings wound around the center of the sample. Assuming a homogeneous flux density distribution within the sample center,

[a]andreas.thul@iem.rwth-aachen.de

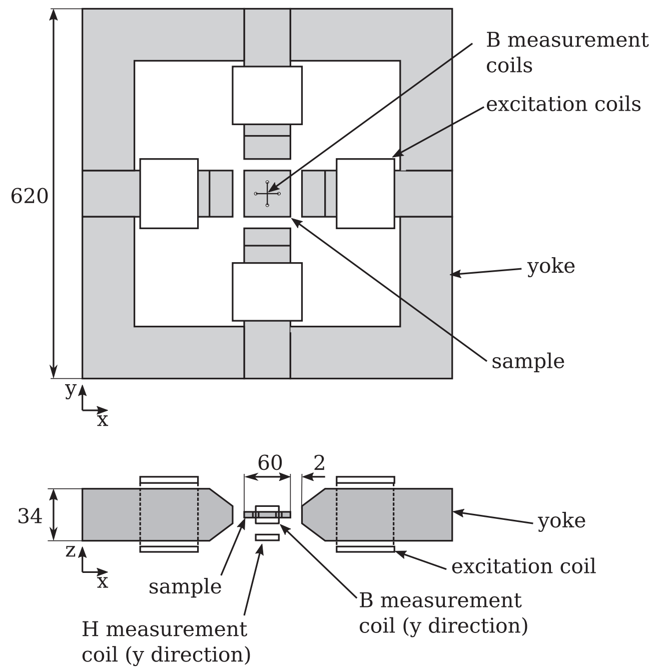

FIG. 1. Top view and cross-section of the RSST measurement system used. (Dimensions given in mm).

the x and y components of the flux density can be calculated from the measured voltages. A homogeneous distribution within the coil can be ensured by choosing the measurement coil width smaller than the sample size.[7] The magnetic field strength is measured by two similar coil systems placed in the air below the sample and extrapolated to the sample surface.

A. Control strategy

To generate a rotating flux distribution inside the sample, the magnitude of the flux density in the measurement region of the sample shall be constant and its direction has to rotate with a given constant angular speed. In this case, the secondary voltages measured in the flux density coils will be sinusoidal with a frequency equal tho the rotating frequency and a phase shift of 90° between x and y axis. Thus, the control objective is to ensure the described secondary voltages by generating suitable excitation voltages in the magnetizing windings. Due to the nonlinear behavior of the material, the excitation voltages will contain harmonics if sinusoidal secondary voltages shall be generated. Usually, two separate waveform control algorithms for each axis are implemented.[6,8,9] Yet both controls are not independent from each other, since a rotating field is to be generated. The control task is similar to rotating electrical machines, where a rotating field has to be controlled as well. This is usually achieved by using field-oriented control strategies based on coordinate transformations, where all quantities are transformed to a virtual rotating winding system. As a result, periodic quantities are transformed to dc quantities, which are easier to control. Therefore, a field-oriented control adapted to RSST is developed here.

1. Coordinate transformation

For electrical machines, various coordinate transformations are possible depending on the specific machine type. Since no mechanically rotating parts exist in RSSTs, any orientation of the virtual winding system is suitable. Here, an alignment of the coordinate system to the reference flux linkage is chosen. The first axis is aligned with the reference flux linkage and called d-axis. The second axis, denoted as q-axis, is perpendicular to the d-axis. Thus the reference d-axis flux density is equal to the reference flux density amplitude, whereas the q-axis flux density reference value is zero.

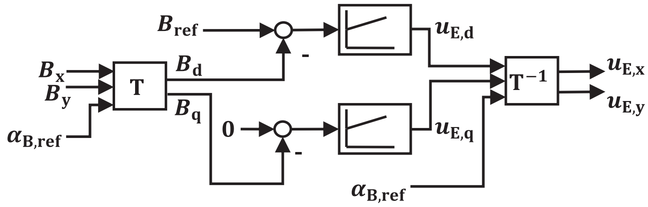

FIG. 2. Structure of the implemented field-oriented control.

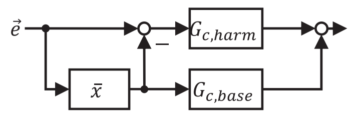

FIG. 3. Separated base frequency and harmonic control principle.

2. Control implementation

For both d- and q-axis, an individual PI control algorithm is implemented as shown in fig. 2. Unlike drive controllers, data acquisition and control operate period-wise. Due to the coordinate transformation, the mean value of any signal is equal to the fundamental frequency component of the untransformed signal. This can be exploited to design two separate controllers in each axis, as shown in fig. 3. One controller is operating only on the mean value and sets the necessary fundamental excitation voltage. The second controller only operates on ac components and thereby reduces undesired flux density harmonics. Both controllers are parametrized independently and adapted depending on the reference flux density and frequency. Additionally, the harmonic controllers are switched off until the base component of the error signal falls under a certain threshold. Thus a fast convergence to the reference value without overshoot or instable behavior is achieved.

III. MEASUREMENT RESULTS AND DISCUSSION

The RSST is used to analyze the material behavior for various grades of electrical steel. This study focuses on non-oriented grades as they are mostly used for electrical machines. A circular flux density rotating in clockwise direction as described in section II A is impressed by the control. In this case loci of the measured flux density vectors will be circles as shown in fig. 4. The magnetization process is then analyzed by examining the corresponding loci of the magnetic field strength. If the sample material was ideally linear and isotropic, the loci of $\vec{H}$ would be circular as well. Due to

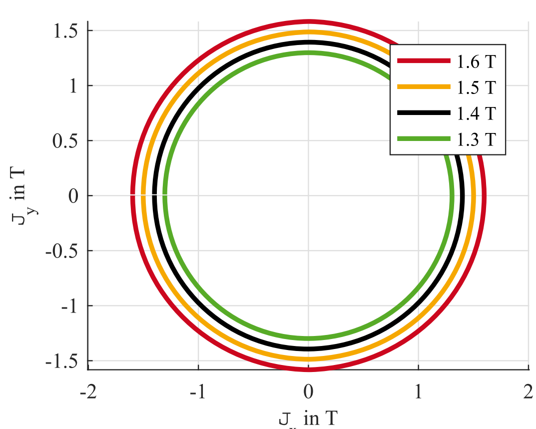

FIG. 4. Loci of $\vec{B}(t)$ for controlled circular polarization. The rolling direction of the sheet sample is aligned to the x axis of the measurement device in all measurements.

TABLE I. Alloying components in wt % for the examined material grades. 'x' denotes an unknown value.

Material	Fe	C	Si	Mn	P	S	Cr	Al
FeSi 24	97.00	0.02	2.42	0.16	0.02	0.01	0.03	0.34
M270-50A	95.67	0.0014	2.9	0.201	0.013	0.0019	-	1.217
M400-50A	x	x	2.376	0.164	x	x	x	0.305

saturation and anisotropy, the actual shape of the $\vec{H}$ loci will not be circular. This will be examined in detail for three materials (FeSi 24-50A, M270-50A and M400-50A, see Table I for chemical compositions).

A. FeSi 24-50A

Fig. 5 shows the $\vec{H}$ loci for different polarization values. This material grade has a small anisotropy, since the necessary magnetic field strength is increased in the transverse direction. Fig. 6 shows the phase angle difference between magnetic field strength and flux density. For small polarizations the reduced permeability influence is visible: Rotating the flux from the rolling to the transverse direction decreases the phase difference between B and H since the field strength has to be increased for magnetizing the transverse direction. Rotating towards the rolling direction on the other hand increases the phase difference. For higher polarizations, this effect is

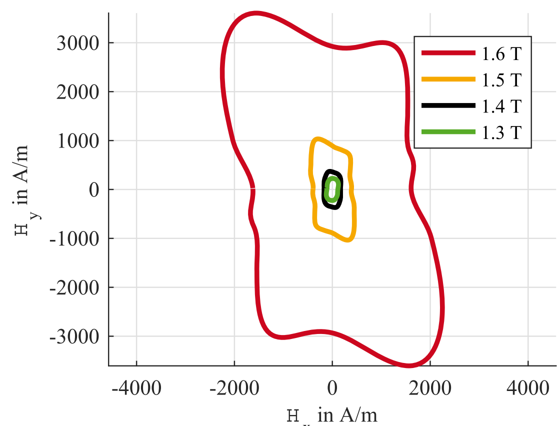

FIG. 5. H loci at circular polarization for the material grade FeSi 24-50A.

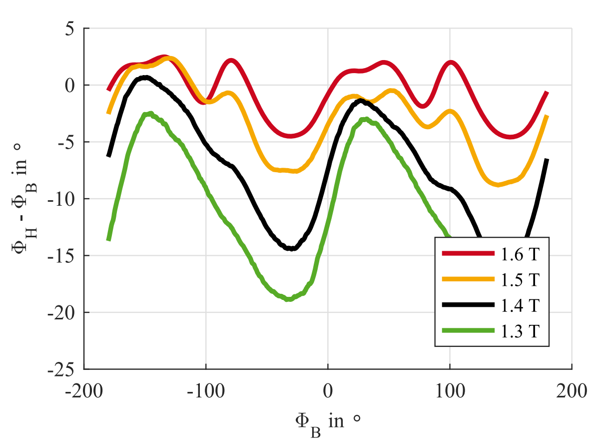

FIG. 6. Phase angle between H and B at circular polarization for the material grade FeSi 24-50A.

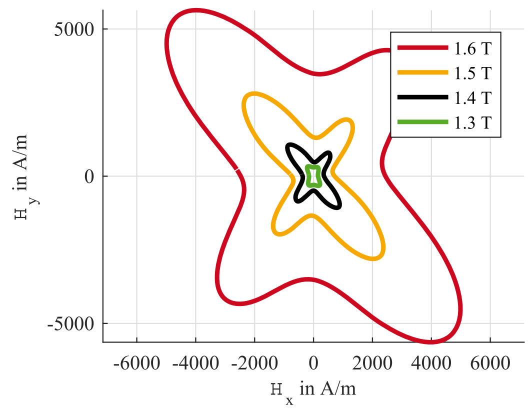

FIG. 7. *H* loci at circular polarization for the material grade M270-50A.

reduced. Further, the different saturation states in both directions additionally influence the phase difference. For the given material saturation becomes the dominant effect for high polarization values.

B. M270-50A

Field strength loci are shown in fig. 7, fig. 8 shows the corresponding phase difference. Compared to the previous material, the anisotropic behavior is more distinctive, similar *H* loci are measured for grain-oriented materials. For small flux densities, the behavior is similar to the previous material FeSi 24, but the influence of anisotropy on the phase angle is increased. For higher flux densities, again anisotropy and saturation both influence the phase difference. In contrast to the previous material, the anisotropy has more influence at high polarization values. As a result, the highest field strength does not occur in the transverse direction as one might expect. Instead, the highest field strength values are reached between both axes.

C. M400-50A

Compared to FeSi 24-50A, the influence of magnetic anisotropy is increased (fig. 9), but the *H* loci do not show the distinctive anisotropic form as measured for M270-50A. Comparing the phase angle difference (fig. 10) indicates a medium grade of magnetic anisotropy compared to the previous materials.

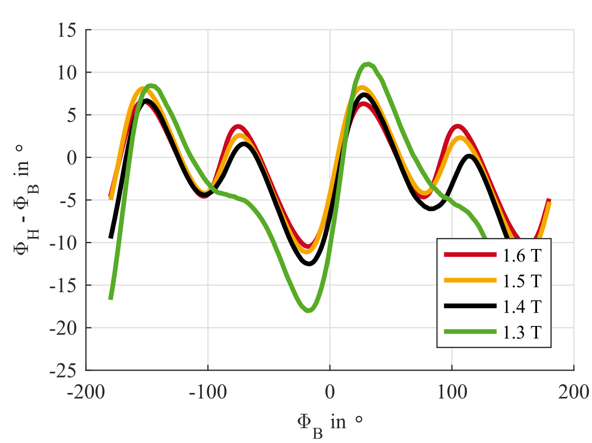

FIG. 8. Phase angle between *H* and *B* at circular polarization for the material grade M270-50A.

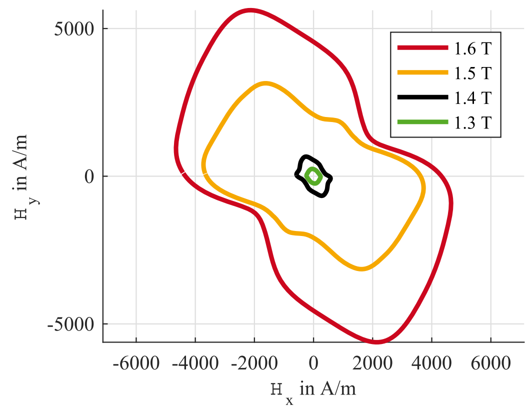

FIG. 9. *H* loci at circular polarization for the material grade M400-50A.

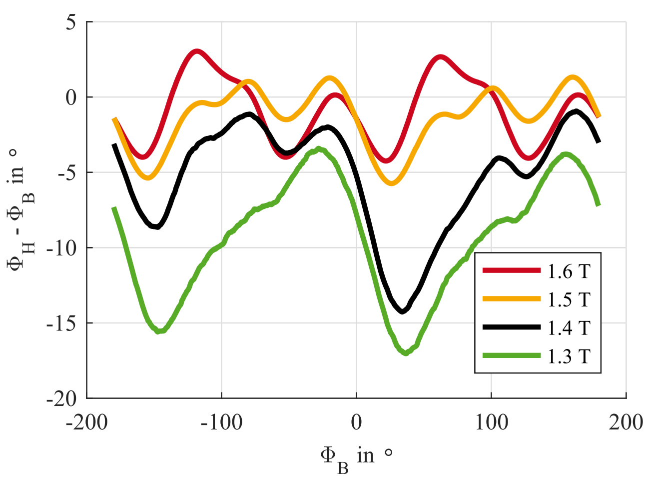

FIG. 10. Phase angle between *H* and *B* at circular polarization for the material grade M400-50A.

IV. CONCLUSION

A four pole RSST is used to examine rotational magnetizations in soft magnetic materials. To improve the feasibility of this measurement technique, a field-oriented control is developed. The results show a significant influence of both anisotropy and saturation on the phase difference between *B* and *H*. All examined non-oriented materials are not completely isotropic. Yet the grade of magnetic anisotropy in those materials can vary considerably. Combined with the saturation influence, this leads to different shapes of H loci. The results emphasize that the vectorial nature of the magnetization process has to be considered. Since standardized measurements use uniaxial magnetization conditions, the presented two-dimensional measurement techniques offer significant advantages. The obtained measurements results can be used for developing and validating suitable material models. Additionally, possible influences of other properties on the magnetization behavior should be examined in the future.

ACKNOWLEDGMENTS

This work is funded by the German Federal Ministry for Economic Affairs and Energy under the Central Innovation Program for SMEs (ZIM) (FKZ: KF 3464501DF4).

[1] S. Steentjes, F. Henrotte, and K. Hameyer, Journal of Magnetism and Magnetic Materials **425**, 20 (2017).
[2] E. Cardelli and A. Faba, Physica B: Condensed Matter **486**, 130 (2016).
[3] Y. Guo, J. G. Zhu, J. Zhong, H. Lu, and J. X. Jin, IEEE Transactions on Magnetics **44**, 279 (2008).
[4] F. Fiorillo and I. D. Mayergoyz, *Characterization and Measurement of Magnetic Materials, Electromagnetism Ser* (Elsevier, Burlington, 2004).
[5] E. Cardelli, A. Faba, M. Pompei, and S. Quondam Antonio, AIP Advances **7**, 056112 (2017).
[6] E. Cardelli, E. Della Torre, A. Faba, and M. Ricci, IEEE Transactions on Magnetics **46**, 3465 (2010).
[7] J. B. Bartolo, P. Klimczyk, K. Tiwisina, P. Denke, S. Siebert, and C. Gerada, International Journal of Applied Electromagnetics and Mechanics **48**, 225 (2005).
[8] D. Makaveev, J. Maes, and J. Melkebeek, IEEE Transactions on Magnetics **37**, 2740 (2001).
[9] Y. Tamura, Y. Ishihara, and T. Todaka, Journal of Magnetism and Magnetic Materials **133**, 382 (1994).